ARTICLE

OBC
www.rsc.org/obc

Peptide backbone folding induced by the C^{α}-tetrasubstituted cyclic α-amino acids 4-amino-1,2-dithiolane-4-carboxylic acid (Adt) and 1-aminocyclopentane-1-carboxylic acid (Ac_5c). A joint computational and experimental study

Massimiliano Aschi,[a] Gino Lucente,*[b,c] Fernando Mazza,[a] Adriano Mollica,[b] Enrico Morera,[b,c] Marianna Nalli[b] and Mario Paglialunga Paradisi[b,c]

[a] *Dipartimento di Chimica, Ingegneria Chimica e Materiali - Università di L'Aquila, I-67100 Coppito, L'Aquila, Italy*

[b] *Dipartimento di Studi Farmaceutici, Università degli Studi di Roma "La Sapienza", P. le A. Moro 5, I-00185 Roma, Italy*

[c] *Istituto di Chimica Biomolecolare, CNR, Sezione di Roma, c/o Dipartimento di Studi Farmaceutici, Università di Roma "La Sapienza", P. le A. Moro 5, I-00185 Roma, Italy*

Received 16th December 2002, Accepted 10th April 2003
First published as an Advance Article on the web 25th April 2003

The conformational study of a new group of synthetic peptides containing 4-amino-1,2-dithiolane-4-carboxylic acid (Adt), a cysteine-related achiral residue, has been carried out through a joint application of computational and experimental methodologies. Molecular Dynamics simulations clearly suggest the tendency of this molecule to adopt a γ-turn conformation in vacuum and help in analyzing the complex and crucial conformational behaviour of the dithiolane ring which appears to preferentially adopt a C_s-like structure. Electronic structure calculations carried out in solution using the Density Functional Theory also indicate the preservation of the γ-like folding in apolar solvents and the helix-like one in more polar solvents. A comparison with the achiral 1-aminocycloalkane-1-carboxylic acid (Ac_5c) has been carried out using the same computational tools. NMR and IR data on dipeptide derivatives containing the Adt or Ac_5c residue show that in chloroform solution all the models prefer a γ-turn structure, centered at the cyclic residue, stabilized by an intramolecular H-bond, whereas in a more polar solvent, *i.e.* dimethyl sulfoxide, this folding is not maintained. The experimental conformational studies, extended to *N*-Boc protected tripeptides, clearly indicate the remarkable tendency of both the five-membered C^{α}-tetrasubstituted cyclic amino acids Adt and Ac_5c to induce the γ-turn structure also in models able to adopt the β-bend conformation.

Introduction

The introduction of C^{α}-tetrasubstituted α-amino acid residues into peptide backbones in order to generate models characterized by reduced conformational flexibility, high tendency to adopt predetermined secondary structures, and enhanced metabolic stability, represents a versatile and well established approach.[1–8] When the biochemical relevance of peptides is considered together with their potential role as therapeutic agents, the importance of an efficient methodology, able to influence the peptide conformational preferences, can be properly evaluated. Based on this approach, potent and selective receptor ligands have been designed and valuable information on the conformation–bioactivity relationships continues to be obtained.[9–14]

Both theoretical and experimental studies on this subject have been published and, in addition to amino acid residues containing two linear side chains bound at the C^{α} carbon atom, the group of C^{α}-tetrasubstituted residues in which the quaternary α-carbon forms part of a ring has been the object of extensive investigation,[15–18] with particular reference to the achiral 1-aminocycloalkane-1-carboxylic acids (Ac_nc, where *n* indicates the number of carbon atoms in the cycloalkane ring).[3] Interest in the cyclic congeners in which one or more heteroatoms form part of the ring is relatively more recent and derives from the potentiality of these amino acid residues to combine, when inserted into the peptide backbone, the tendency to stabilize specifically folded conformers with the establishment of intra- or inter-molecular interactions through the side chain functionality.[19–21] In this field we reported recently[22] a study concerning a γ-turn conformation induced by two six-membered C^{α}-tetrasubstituted cyclic amino acids, namely: 4-amino-tetrahydrothiopyran-4-carboxylic acid (Thp), containing a sulfur atom in the ring, and the related cycloaliphatic model 1-aminocyclohexane-1-carboxylic acid (Ac_6c). Computational observations carried out on the model Ac-Thp-NHMe showed that a γ-turn represents the lowest minimum; at the same time ^{1}H-NMR and IR studies, performed on the dipeptide derivatives HCO-Thp-Leu-OMe and HCO-Ac_6c-Leu-OMe, showed that such a conformation is retained in $CDCl_3$ whereas it is lost in the more polar $(CD_3)_2SO$ solvent.

The γ-turn conformation involves three consecutive amino acid residues and can be stabilized by an intramolecular H-bond between the CO of the first residue (*i*) and the NH of the third residue (*i*+2) forming a seven-membered ring. As shown in Fig. 1, γ-turn and inverse γ-turn are characterized by different ϕ^{i+1} and ψ^{i+1} torsion angles. Although less frequent than β-turn, the γ-turn secondary structure is thought to play important roles in molecular recognition,[23–27] and the presence of γ-turn in solution of several bioactive peptides has been proposed.[28]

As a part of our continuing interest in the field of heterocyclic α-amino acids containing a quaternary α-carbon atom we started recently[19,20] a study on a new group of synthetic peptides containing 4-amino-1,2-dithiolane-4-carboxylic acid (Adt), a cysteine-related achiral residue, characterized by the presence of a five-membered ring in which a disulfide function is contained. Although 1,2-dithiolanes can be easily obtained by mild oxidation from the corresponding 1,3-dithiols, their chemical reactivity is clearly distinct from that of linear and

DOI: 10.1039/b212247b

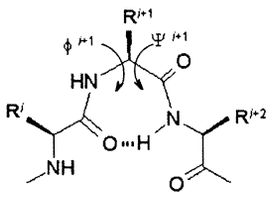

Fig. 1 Schematic representation of γ-turn and inverse γ-turn conformations.

larger ring 1,2-disulfides and represents the key structural feature on which the activity of relevant biomolecules, such as lipoic acid, is based;[29] thus, the study of the properties of synthetic peptides containing this residue appears of general interest. Here we report a joint computational and experimental study on the property as γ-turn inducer of the cyclic C^{α}-tetrasubstituted α-amino acid Adt and of the structurally related Ac_5c which contains, as compared with the Adt residue, a $–CH_2–CH_2–$ unit in place of the disulfide function.

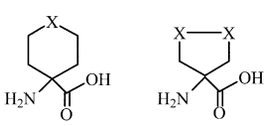

In the first part of the work an exhaustive computational analysis of the energetic and structural features of Adt and Ac_5c is addressed both in vacuum and in solution; a combined application of classical Molecular Dynamics (MD) simulations and quantum-chemical calculations is used for this purpose. In the second part of the work a solution conformational analysis of Adt- and Ac_5c-containing peptide models, aimed at evaluating the theoretical predictions on the experimental data, is reported.

Results and discussion

1. Dynamic Reaction Path calculations

A preliminary analysis of the conformational features of the C^{α}-tetrasubstituted achiral residue Adt in vacuum was performed through MD simulations. In the model examined (Ac-Adt-NHMe) the N and C ends are protected by the CH_3CO and NHMe groups, respectively.

The MD simulation represents a valuable tool for exploring the properties of the potential energy hypersurface of a system showing a relatively high number of internal degrees of freedom such as the Ac-Adt-NHMe molecule here under study. In particular the aim is to evaluate the preferred conformation of the dithiolane ring, together with the ϕ and ψ values, adopted by the Ac-Adt-NHMe molecule at the equilibrium. To this end we adopted the DRC[30] approach which produces a classical trajectory by calculating, step by step, the potential energy and its analytical gradient through quantum chemical procedures. In the present case, the semiempirical AM1 Hamiltonian[31] was adopted for energy and gradient calculations. It must be remarked that, unlike the classical MD simulations with predefined force fields, the DRC simulations which build the forces acting on each atom using quantum mechanics, are computationally rather demanding and hence can hardly be extended for times longer than 20–30 ps.

Two trajectories, propagated at constant energy and angular momentum, were initiated with a Maxwellian distribution of the velocities corresponding to a starting temperature of 298 K. The first trajectory was started assuming for Ac-Adt-NHMe a conformation close to a helical structure with $\phi = 61°$ and $\psi = 16°$; an almost opposite conformation with $\phi = -60°$ and $\psi = -20°$ was the starting point of the second trajectory. Both the starting structures correspond to high-energy conformations having the CSSC torsion angle as large as 24°. This choice ensures, during the energy-constant simulation, a sufficient amount of internal energy allowing one to span the ϕ/ψ and the CSSC conformational space as much as possible.

The obtained trajectories were initially analyzed in terms of their root mean square deviation (rmsd) with respect to the starting structures. Such analysis provides the primary tool for assessing when and how the system under investigation reaches the actual equilibrium. Both runs revealed equilibration not before 9.0 ps. After such a time the rmsd reaches a constant value. Therefore the portion of the trajectory before such a point is disregarded in the following analysis. Fig. 2 shows the distribution of the CSSC torsion angle sampled in the last 9 ps of each trajectory. It is evident that at the dynamic equilibrium, the Adt ring adopts a CSSC torsion angle oscillating around 0° and that the ring conformations displacing from this value play no significant role.

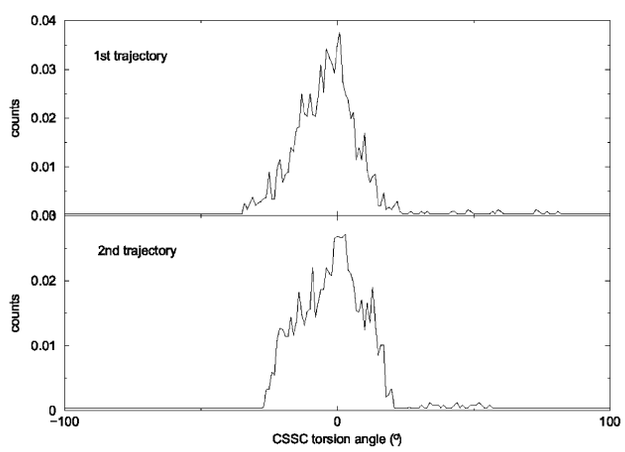

Fig. 2 Distribution of the CSSC torsion angle along the last 9 ps of each trajectory.

Both the trajectories were then projected on the ϕ–ψ map, generating a 'dynamic' Ramachandran map shown in Fig. 3. The Ac-Adt-NHMe preferentially adopts the γ-turn conformations. Moreover, it should be remarked that the two γ-turns never interconvert, *i.e.* the two trajectories never appear to

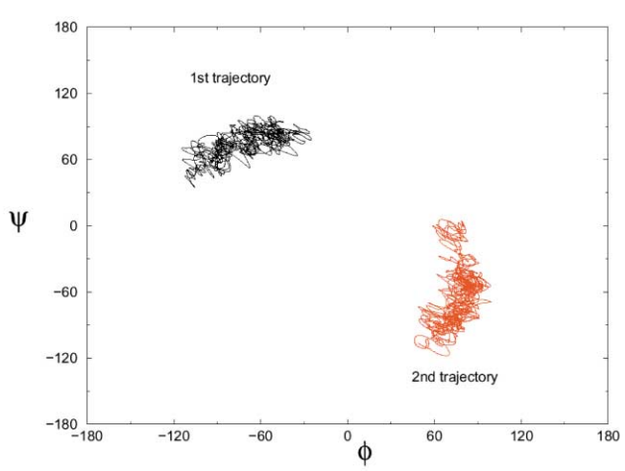

Fig. 3 Dynamic Ramachandran plot reported as count of the ϕ and ψ values sampled along the last 9 ps of the trajectories.

Table 1 Potential energy differences (E) including Zero Point Energy and selected geometrical parameters for the most relevant minima in vacuum of the Ac-Adt-NHMe and Ac-Ac$_5$c-NHMe species calculated at the B3LYP/6-31G(d)//B3LYP/4-31G level of theory

Ac-Adt-NHMe

Species	Type	E/kJ mol^{-1}	ϕ/°	ψ/°	NH–O/Å	N–H–O/°	CSSC/°	τ/°
I	γ	0	−72.8	55.3	1.800	152.3	5.3	113.5
II	iγ	0	72.3	−55.7	1.802	152.3	−6.3	113.5
III	f.e.	4.6	179.3	−162.5	1.960	114.9	2.6	103.5
IV	α_R	6.7	−70.0	−20.5	—	—	4.4	113.1
V	α_L	6.7	70.1	20.5	—	—	−4.4	113.1

Ac-Ac$_5$c-NHMe

Species	Type	E/kJ mol^{-1}	ϕ/°	ψ/°	NH–O/Å	N–H–O/°	CCCC/°	τ/°
I	γ	0	74.2	−60.9	1.870	149.4	−9.2	111.3
II	iγ	0.4	−72.8	55.4	1.849	151.8	−12.4	112.3
III	f.e.	3.3	178.9	177.6	1.989	113.8	39.6	104.0
IV	α_R	6.3	−73.9	−14.2	—	—	−1.9	112.3
V	α_L	6.3	73.8	14.2	—	—	1.9	113.4

mutually superimpose. This could be ascribed to the presence of a relatively large barrier created by the overlapping involving the carbonyl oxygen of the acetyl group and the amide hydrogen atom of the terminal NHMe.

In conclusion, this preliminary analysis reveals for Ac-Adt-NHMe in vacuum two deep not mutually interconverting minima, corresponding to the γ-turn and inverse γ-turn conformations both adopting an almost *cis*-planar CSSC torsion angle.

2. DFT calculations in vacuum

The information on the Born–Oppenheimer surface previously obtained by the MD run was then used as a starting point for addressing the energetic and structural features of Adt at a more sophisticated level of theory. Thus, the Density Functional Theory (DFT), which has been shown to be able to describe the subtle effects governing the conformational equilibria in peptides,[32] was applied. In particular, on the basis of the MD run, we re-sampled in vacuum the preferred regions of the potential energy surface of Adt by using the B3LYP functional in conjunction with split valence basis sets (see computational details). The related results are reported in Tables 1 and 2. In the same Tables we also report analogous calculations carried out on the Ac-Ac$_5$c-NHMe model which refer to the Ac$_5$c ring. The analysis of the two sets of calculations should reveal possible differences between the heterocyclic and the cycloaliphatic ring systems, *i.e.* possible differential effects of the nature of the ring on the conformer population.

Five deep potential energy minima, energetically close to each other, have been found at the DFT level of theory for both species. In the case of Ac-Adt-NHMe, in accordance with the previous DRC results, the two lowest minima correspond to the γ-turn and inverse γ-turn (iγ) structures, respectively. The third one is associated with the fully extended (f.e.) conformation, while helices (α_R and α_L) appear as the last two minima lying 6.7 kJ mol^{-1} above the γ-turns. Such a result is paralleled by the intramolecular H-bond formation. As can be seen in Table 1, an H-bond is present in both the γ-turns (H–O = 1.80 Å, NH–O angle = 152°) and it is also present in the f.e. conformation, although with a longer contact (H–O = 1.96 Å) and a smaller linear character (NH–O angle = 115°); no H-bonds are possible in the two helical conformations. It is also interesting to observe that all the above minima are associated with an almost *cis*-planar CSSC torsion angle, ranging between 5.3° and −6.3°. It must also be remarked that, as already suggested by MD calculations, widening of the CSSC value causes an increase of the potential energy leading to high-energy structures and to first and higher order saddle points whose geometrical and energetic features are not reported. Moreover, the f.e. structure appears as the third minimum despite a valence angle as large as 103.5°, significantly distorted from the tetrahedral value.

The results referring to Ac-Ac$_5$c-NHMe are rather similar to those obtained for Ac-Adt-NHMe. At variance with the Adt model, the f.e. conformer presents a more puckered pentaatomic ring with the torsion angle, opposite to the C$^\alpha$ atom, of +39.6°. The conformer population is finally evaluated for both Ac-Ac$_5$c-NHMe and Ac-Adt-NHMe in the ideal gas approximation using the free energy differences reported in Table 2. The results are reported in Fig. 4 and show that, at the DFT level, at 298 K, the γ-turn conformers are the most populated. This should be entirely ascribed to the enthalpic gain due to the intramolecular H-bond, since the entropy contribution remains basically the same for all the conformers.

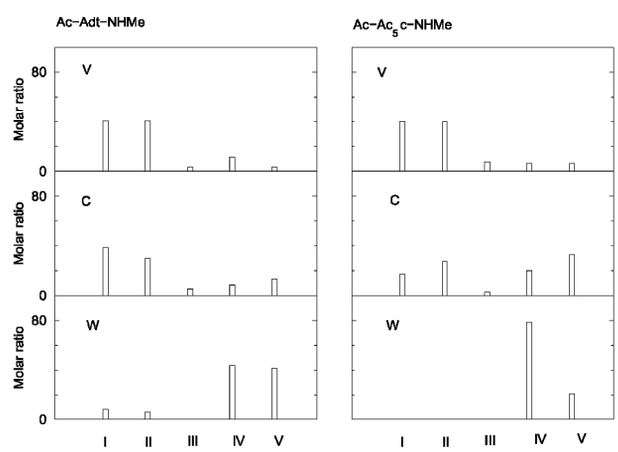

Fig. 4 Room temperature molar ratios in vacuum (V), chloroform (C) and water (W) for the thermodynamically more accessible species of Adt and Ac$_5$c (see text) calculated using Density Functional Theory. The roman numbers are those of Table 1.

3. DFT calculations in solution

The effect of the solvent was also addressed by carrying out the previous DFT calculations in solution by using the polarizable continuum model[33,34] in two completely different solvents, in order to evaluate the influence of the polarity of the medium on the conformer relative stabilities.

The results are also reported in Tables 1 and 2. From a structural point of view, none of the geometrical features undergo large modifications with respect to the vacuum. For

Table 2 298 K Gibbs free energy differences in vacuum (ΔGv). 298 K solvation Gibbs free energies in chloroform (ΔGc) and in water (ΔGw) calculated at the B3LYP/6-31G(d)//B3LYP/4-31G level of theory. These values are reported in bold type. The electrostatic, dispersion–repulsion and cavitation contributions to the solvation free energies (see text) are reported in italics

Ac-Adt-NHMe

Species	ΔGv/kJ mol^{-1}	ΔGc/kJ mol^{-1}	ΔGw/kJ mol^{-1}
I	**0**	**−8.8**	**−39.3**
		−14.6	*−53.6*
		−73.2	*−96.7*
		+79.0	*+111.0*
II	**0**	**−8.2**	**−36.8**
		−14.2	*−51.5*
		−73.7	*−96.7*
		+79.3	*+111.4*
III	**+3.1**	**−6.9**	**−27.6**
		−14.6	*−41.7*
		−73.2	*−97.5*
		+80.9	*+111.6*
IV	**+6.3**	**−11.3**	**−44.8**
		−19.2	*−61.5*
		−73.2	*−96.3*
		+81.1	*+113.0*
V	**+6.3**	**−12.3**	**−51.5**
		−20.1	*−67.8*
		−73.2	*−96.3*
		+81.0	*+112.6*

Ac-Ac$_5$c-NHMe

Species	ΔGv/kJ mol^{-1}	ΔGc/kJ mol^{-1}	ΔGw/kJ mol^{-1}
I	**0.4**	**−8.4**	**−31.0**
		−14.2	*−46.9*
		−69.1	*−90.8*
		+74.9	*+106.7*
II	**0**	**−9.6**	**−37.2**
		−16.7	*−51.9*
		−69.3	*−90.8*
		+76.4	*+105.5*
III	**+4.6**	**−13.4**	**−54.4**
		−22.2	*−72.0*
		−69.1	*−90.0*
		+77.9	*+107.6*
IV	**+4.6**	**−14.6**	**−51.1**
		−23.4	*−68.2*
		−68.6	*−90.0*
		+77.4	*+107.1*
V	**+4.2**	**−7.9**	**−35.6**
		−13.8	*−49.8*
		−69.9	−92.1
		+75.8	*+106.3*

this reason they have not been explicitely reported. On the other hand, from the energetic point of view, the inclusion of the bulky-solvent effect appears to sharply affect the relative population of the conformers. Fig. 4 shows that the 298 K conformers, poorly populated in vacuum, become thermodynamically more accessible in solution. For example, in chloroform the γ-turn remains thermodynamically populated but, on the other hand, the helical structures increase their stability.

In this context it can be noted that Ac-Adt-NHMe shows some differences with respect to Ac-Ac$_5$c-NHMe. In fact, while the γ-turns appear as the most populated structures in chloroform in the case of Ac-Adt-NHMe, in the same solvent Ac-Ac$_5$c-NHMe preferentially adopts a helical structure (see Fig. 4). From the collection of the free energy contributions reported in Table 2, the systematically larger dispersion–repulsion term does probably play a key role in such a difference in chloroform. Interestingly, what must also be remarked is the disappearance of the f.e. structures which can probably be ascribed to an increase in the stability of γ-turn and helical structures.

In a more polar solvent, such as water, we essentially do not observe large differences between the two species. The helical structures, owing to their enhanced ability to expose the polar groups to the solvent,[32] become the most stable conformations, whereas both the γ-turns and the f.e. conformers practically disappear at the same temperature. The presence of explicit water molecules would probably enhance such an effect[32] which, on the basis of the presently employed model, has to be entirely ascribed to averaged bulk effects.

In conclusion, the dithiolane ring does favour the adoption of a γ-turn-like conformation in apolar solvents where the intramolecular hydrogen bond is the driving force for the adoption of the conformations. When, on the other hand, the polarity of the medium is increased, the helical structure, which allows the polar groups to be better solvent-exposed, becomes preferred. Interestingly, the present computational results suggest that the disulfur containing ring, when compared to Ac$_5$c, slightly favours the adoption of a γ-turn conformation with respect to the helical one, both in vacuum and in apolar solvents.

4. Chemistry

The synthesis of dipeptides Boc-Adt-Leu-OMe (**1a**), Boc-Ac$_5$c-Leu-OMe (**1b**), HCO-Adt-Leu-OMe (**2a**), and HCO-Ac$_5$c-Leu-OMe (**2b**), and of tripeptides Boc-Adt-Leu-Ala-OMe (**3a**) and Boc-Ac$_5$c-Leu-Ala-OMe (**3b**), was performed according to Scheme 1. **1a** and **1b** were prepared by coupling Boc-Adt-OH or Boc-Ac$_5$c-OH with H-Leu-OMe by the HOBt–EDC method. The above carbodiimide procedure was also employed to obtain the tripeptides **3a** and **3b**, although different strategies were adopted: in the case of **3a** the dithiolanic derivative Boc-Adt-OH was coupled with the dipeptide H-Leu-Ala-OMe, while the Ac$_5$c-containing tripeptide **3b** was prepared from Boc-Ac$_5$c-Leu-OH and H-Ala-OMe. A direct transformation of the *N*-Boc derivatives **1a**,**b** into the corresponding *N*-formyl analogs **2a**,**b** was performed by following the procedure of Lajoie and Kraus[35] by treatment with formic acid, followed by EEDQ.

5. Solution conformation

In order to probe whether the γ-turn preference, previously inferred through computational methods for Ac-Adt-NHMe and Ac-Ac$_5$c-NHMe models, is maintained in $CDCl_3$ solution, a ^{1}H NMR and IR conformational analysis of compounds **1**–**3** was undertaken. The assignment of the NH resonances in Boc-protected dipeptides **1a** and **1b** is straightforward: the Adt and Ac$_5$c NH groups resonate as singlets at higher field than the Leu NH which appears in **1a** as a doublet (J = 8 Hz) and in **1b** as a broad signal. The involvement of the NH groups in intramolecular hydrogen bonds was evaluated on the basis of the chemical shift solvent dependence in $CDCl_3$–$(CD_3)_2SO$ mixtures. As shown in Figs. 5A and 5C, the Adt and the Ac$_5$c NH groups are significantly more sensitive to changes in solvent composition as compared with the Leu NH group which appears strongly solvent shielded. This behaviour clearly indicates that the Leu NH is not accessible to the solvent in both Boc dipeptides **1a** and **1b** and is presumably involved in an intramolecular hydrogen bond, while the Adt and Ac$_5$c NH groups are solvent exposed.

In order to confirm the above reported results, the IR spectra in $CHCl_3$ in the NH stretching region of **1a** and **1b** were examined. As is well known, a free amide NH gives rise to a sharp absorption in the 3400–3470 cm^{-1} domain and is shifted in the 3300–3800 cm^{-1} region by hydrogen bonding.[36,37] In the spectrum of **1a** two bands are observed at 3306 and 3419 cm^{-1}, corresponding to the H-bonded and free NH groups, respectively. The ratio between the intensity of the two absorptions

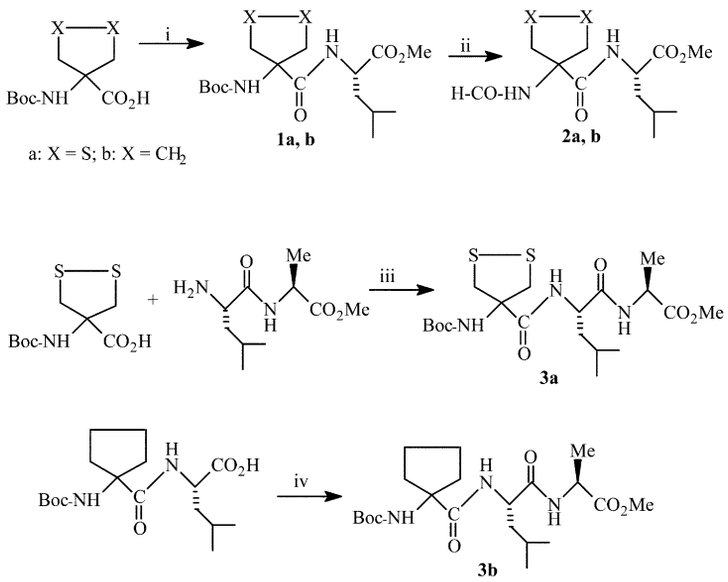

Scheme 1 *Reagents and conditions*: i: HOBt, EDC, H-Leu-OMe·HCl, DMF; ii: HCOOH, EEDQ; iii: HOBt, EDC, TEA, DMF; iv: HOBt, EDC, H-Ala-OMe, TEA, DMF.

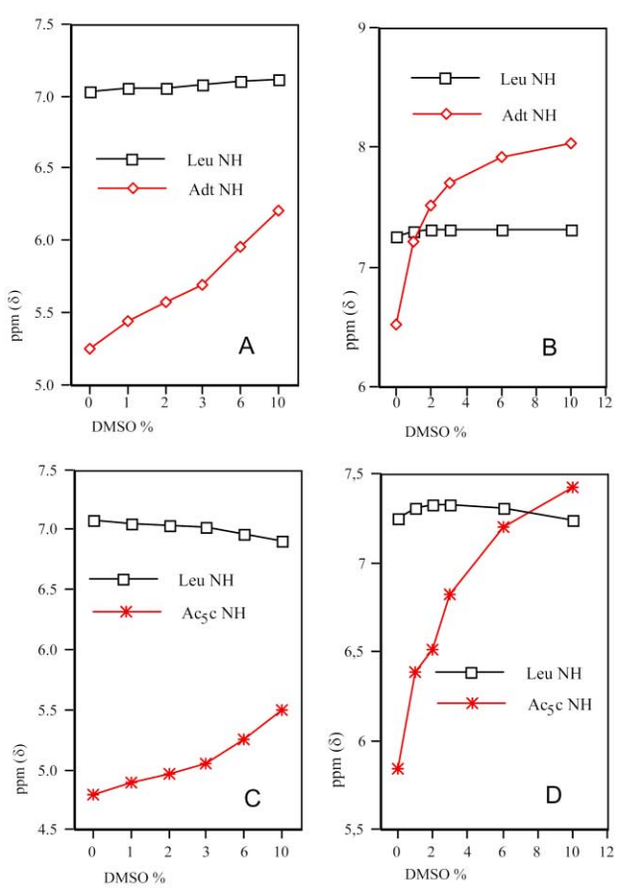

Fig. 5 Chemical shift dependence of the NH resonances as a function of the DMSO-d_6 concentration (% v/v) in $CDCl_3$ solution. A: *N*-Boc-Adt-Leu-OMe (**1a**); B: HCO-Adt-Leu-OMe (**2a**); C: *N*-Boc-Ac_5c-Leu-OMe (**1b**); D: HCO-Ac_5c-Leu-OMe (**2b**). Peptide concentration 10 mM.

was found to be practically concentration independent over the range 10 to 1.0 mM. Thus, peptide self-association occurs, if at all, to a limited extent under these experimental conditions and the band at 3306 cm^{-1} can be assigned to the intramolecularly H-bonded Leu NH group. The IR spectrum of **1b** shows a very close outcome in the NH stretching region: two bands are observed at 3308 and 3436 cm^{-1}, and the band at lower frequency can be assigned to intramolecularly bonded Leu NH.

Table 3 Observed nuclear Overhauser effects (NOEs) in the NOESY spectra of Boc-Adt-Leu-OMe (**1a**) and Boc-Ac_5c-Leu-OMe (**1b**)[a]

1a		**1b**	
Leu NH ··· Adt NH	m	Leu NH ··· Ac_5c NH	m
Leu NH ··· Leu $C^{\alpha}H$	m	Leu NH ··· Leu $C^{\alpha}H$	m
Leu $C^{\alpha}H$ ··· Leu $C^{\beta}H_2$	s	Leu $C^{\alpha}H$ ··· Leu $C^{\beta}H_2$	s
Adt NH ··· Adt CH_2	w and s	Ac_5c NH ··· Ac_5c $C^{\beta}H_A$[b]	s
Leu NH ··· Adt CH_2	w	Leu $C^{\alpha}H$ ··· Leu $C^{\delta}H_3$	w
Leu $C^{\alpha}H$ ··· Leu $C^{\delta}H_3$	w	Leu NH ··· Leu $C^{\beta}H_2$	s
Leu NH ··· Leu $C^{\beta}H_2$	s		

[a] s, strong; m, medium; w, weak. [b] $C^{\beta}H_A$ protons (see Fig. 6) resonate at higher field than $C^{\beta}H_B$.

Although the position of the NH absorptions cannot be unequivocally associated with specific folded structures,[12] it should be noted that the stretching bands of intramolecularly H-bonded Leu NH of **1a** and **1b** occur at frequencies very close to those observed for the same group in the related dipeptides HCO-Ac_6c-Leu-OMe and HCO-Thp-Leu-OMe,[22] which adopt the γ-turn conformation.

All these findings, which are in accordance with the above reported computational results, indicate that a significant population of conformers of the two dipeptides **1a**,**b** adopts, in $CDCl_3$ solution, a folded γ-turn conformation characterized by an H-bond interaction between the Leu NH and the urethanic carbonyl group.

Further information on the conformation adopted by the *N*-Boc dipeptides **1a**,**b** can be obtained by examining the results of nuclear Overhauser effect (NOE) experiments summarized in Table 3. The observation of an NH ··· NH cross-peak corresponding to close contact of the Adt and Leu NH protons confirms that **1a** adopts a folded γ-turn structure centered at the Adt residue. An analogous spatial connectivity is shown by the Ac_5c and Leu NH groups of related *N*-Boc dipeptide **1b**. A further diagnostic feature in the NOESY spectrum of **1b** concerns the strong NOEs between the Ac_5c NH and the four adjacent ring protons (see Table 3 and Fig. 6): a strong effect is observed only with the pair of protons $C^{\beta}H_A$ which resonate at higher field as compared with the $C^{\beta}H_B$ protons. This is in accordance with the presence of a γ-turn conformation in which the Ac_5c NH shows a large interproton distance only with the $C^{\beta}H_B$ pair; the two $C^{\beta}H_B$ protons lie in fact on the opposite side of the ring and experience a selective deshielding by the cisoidal Ac_5c amide carbonyl group. A similar outcome

Table 4 Solvent accessibility of peptide NH groups: differences ($\Delta\delta$, ppm) between NH chemical shift values observed in $CDCl_3$ solution containing $(CD_3)_2SO$ (10%) and in neat $CDCl_3$; see also Figs. 5 and 7

Compound	Adt or Ac_5c NH	Leu NH	Ala NH
Boc-Adt-Leu-OMe (**1a**)	0.95	0.09	
Boc-Ac_5c-Leu-OMe (**1b**)	0.70	−0.17	
Boc-Adt-Leu-Ala-OMe (**3a**)	1.00	0.26	0.62
Boc-Ac_5c-Leu-Ala-OMe (**3b**)	0.82	0.01	0.35
HCO-Adt-Leu-OMe (**2a**)	1.51	0.06	
HCO-Ac_5c-Leu-OMe (**2b**)	1.57	0.005	
Thp or Ac_6c NH			
HCO-Thp-Leu-OMe[a] (**4**)	2.01	0.12	
HCO-Ac_6c-Leu-OMe[a] (**5**)	1.72	0.12	

[a] Ref. 22.

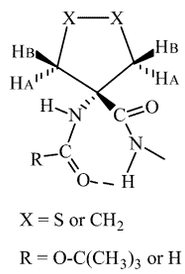

Fig. 6 Intramolecularly H-bonded γ-turn structure of dipeptides **1a**, **2a** (X = S) and **1b**, **2b** (X = CH_2).

is exhibited by the Adt-containing dipeptide **1a**; however, the partial overlapping of the Adt $C^{\beta}H_A$ and $C^{\beta}H_B$ signals does not allow, in this case, an exact evaluation of the Adt NH ··· CH_2 connectivity; this finding could reflect the different conformations adopted by the two five-membered rings.

The above reported results of ^{1}H-NMR solvent shielding experiments can be usefully compared with those previously obtained by us when studying the two *N*-formyldipeptide models HCO-Thp-Leu-OMe (**4**) and HCO-Ac_6c-Leu-OMe (**5**), both containing a cyclic C^{α}-tetrasubstituted achiral residue at the *N*-terminal position and exhibiting a tendency to adopt a γ-turn conformation centered at the cyclic residue.[22] For this purpose we have summarized in Table 4 the differences ($\Delta\delta$, ppm) between the NH chemical shifts observed in $CDCl_3$ containing 10% $(CD_3)_2SO$ and in neat $CDCl_3$. It can be seen that the Leu NH shows, as expected for intramolecularly bonded protons, low $\Delta\delta$ values for both the *N*-Boc dipeptides (**1a** and **1b**) here under study as well as for the two previously studied *N*-formyldipeptides **4** and **5**. It can be observed, however, that in the case of the *N*-Boc dipeptides **1a** and **1b** the Adt and Ac_5c NH groups show $\Delta\delta$ values significantly lower than those exhibited by the corresponding Thp and Ac_6c NH of the previously studied *N*-formyldipeptides (*i.e.*: 0.95 and 0.70 ppm in the case of urethanic Adt and Ac_5c NH, respectively; 2.01 and 1.72 ppm for the Thp and Ac_6c formamido NH groups in **4** and **5**, respectively). This finding indicates that the bulkiness of the Boc protecting group in **1a**,**b** and **3a**,**b** may significantly contribute to lowering the solvent accessibility shown by the corresponding NH group. In order to get information on this point, the related *N*-formyl derivatives **2a**,**b** were synthesized and examined. Data reported in Figs. 5B and 5D and Table 4 show that the Adt and the Ac_5c formamido NH groups of **2a**,**b** exhibit higher $\Delta\delta$ values (1.51 and 1.57 ppm, respectively) than those observed for the corresponding Boc-protected NH groups of **1a** and **1b** (0.95 and 0.70 ppm, respectively). This confirms that the lower sensitivity of chemical shift to the solvent composition exhibited by urethanic NH protons of **1a** and **1b** is connected with the different steric dimensions of the substituents at the NH groups.

The above described titration experiments were then extended to tripeptides Boc-Adt-Leu-Ala-OMe (**3a**) and Boc-Ac_5c-Leu-Ala-OMe (**3b**). As shown in Fig. 7 and Table 4, in

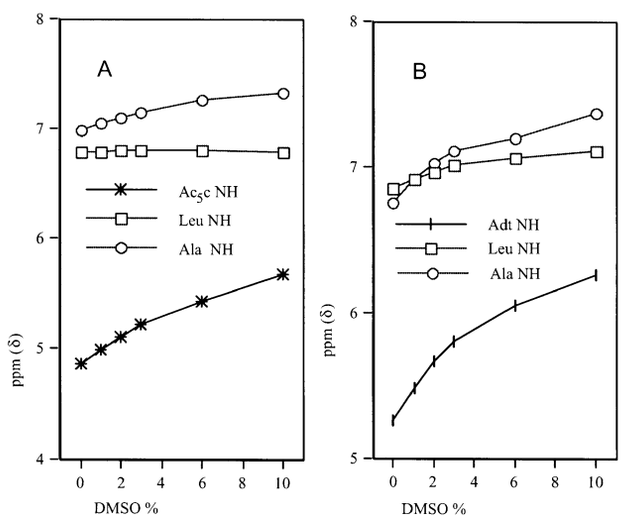

Fig. 7 Chemical shift dependence of the NH resonances as a function of the DMSO-d_6 concentration (% v/v) in $CDCl_3$ solution. A: *N*-Boc-Adt-Leu-Ala-OMe (**3a**); B: *N*-Boc-Ac_5c-Leu-Ala-OMe (**3b**). Peptide concentration 10 mM.

both these derivatives the urethane NH resonance moves downfield with increasing concentration of $(CD_3)_2SO$, while the Leu NH group is practically unaffected by the change of the solvent composition. An intermediate behaviour is observed in the case of the Ala NH. These results confirm the tendency of Adt and Ac_5c residues to induce, in $CDCl_3$ solution, γ-turn conformations centered at the cyclic residue also in peptides able to adopt β-bend structures. The intermediate solvent accessibility shown by Ala NH (see Table 3) can be explained by admitting the presence of a certain population of a β-turn or a double γ-turn centered at the first two residues. Unfortunately, in the NOESY spectra of both the tripeptides **3a**,**b** the overlapping of Leu and Ala $C^{\alpha}H$, together with the close resonances of the corresponding NH groups, does not allow the observation of the related diagnostic spatial connectivities. Further information which can be obtained by examining the $\Delta\delta$ values reported in Table 4 concerns an evaluation of the relative tendency to stabilize a γ-turn folding exhibited by the Adt and Ac_5c residues. It can be seen that the $\Delta\delta$ values of the γ-turn involved Leu NH protons show, in all three Ac_5c-containing peptides **1b**–**3b**, a value lower than that exhibited by the corresponding Adt-containing models **1a**–**3a**. This strongly suggests that, although both the cyclic residues induce the γ-turn folding, the tendency associated with the Ac_5c presence is more pronounced. This behaviour is not found in the case of the cyclic residues of Thp and Ac_6c in which (see Table 4) the Leu NH presents the same $\Delta\delta$ value.

Finally, in order to check whether a dipolar solvent could disfavour the γ-turn conformations observed in $CDCl_3$ solution, NOESY experiments have been carried out on

formyldipeptides **2a** and **2b** in $(CD_3)_2SO$ solution. Only a weak Leu NH ··· Adt NH cross-peak was observed in the spectrum of **2a**, and the corresponding spatial connectivity between Leu and Ac_5c NH groups of **2b** could not be detected. Furthermore, the Leu NH group of both the formyldipeptides **2a** and **2b** exhibit, in $(CD_3)_2SO$, relatively high temperature coefficients (0.0051 ppm K^{-1} and 0.0043 ppm K^{-1}, respectively). These data strongly suggest that the folded γ-turn structure adopted by **2a** and **2b** in $CDCl_3$ solution is not retained in the polar solvent.

Conclusions

NMR and IR data on the conformations adopted by dipeptides containing the Adt (**1a** and **2a**) or the Ac_5c (**1b** and **2b**) residue at the *N*-terminal position, reported in the present paper, show that in chloroform solution all the models prefer a γ-turn structure stabilized by an intramolecular H-bond (see Fig. 6); this folding is not maintained in a polar solvent such as dimethyl sulfoxide, where linear intermolecular H-bonding interactions with the medium prevent the formation of the γ-turn structure. The experimental conformational studies, performed in $CDCl_3$ solution, were extended to the *N*-Boc-protected tripeptides **3a** and **3b** and the results obtained indicate the remarkable tendency of both the five-membered C^{α}-tetrasubstituted cyclic amino acids Adt and Ac_5c to induce the γ-turn structure also in models able to adopt the β-bend conformation. An analogous behaviour was previously observed in the case of models containing six-membered C^{α}-tetrasubstituted cyclic amino acids Thp and Ac_6c.[22] The present results are in good agreement with the conformational energy and free-energy calculations performed on the Ac-Adt-NHMe and Ac-Ac_5c-NHMe models. However, while the computational data suggest that the Adt residue, when compared to the Ac_5c, is a more efficient γ-turn inducer, both in vacuum and in apolar solvents, the spectral data indicate that the tendency to induce this folding is more pronounced in the case of the Ac_5c residue. Such a discrepancy is probably due to the well known limitations in the theoretical description of the solutions ranging from the absence of explicit solvent molecules to the impossibility of calculating an exact molecular partition function, which obviously lower the performances and the accuracy normally reached in the gas phase by standard theoretical models.

Experimental

Dynamic Reaction Path calculations

Dynamic Reaction Path calculations were carried out using the implementation of Gordon and Taketsugu present in the package Gamess US.[38] The trajectories were subsequently analyzed with our own routines interfaced with the above package. The initial system is 'heated' up to a Maxwellian distribution of 298 K and then allowed to propagate and equilibrate using a velocity-Verlet[39] algorithm with a time step of 0.1 fs by keeping constant the energy and the angular momentum. Both the trajectories were stopped after about 150 000 steps. The AM1 level of theory[31] was adopted for the energy and gradient calculations.

Density Functional Theory calculations

The Born–Oppenheimer potential energy hypersurfaces of Ac-Adt-NHMe and Ac-Ac_5c-NHMe were fully investigated without any geometrical constraint in the framework of the Density Functional Theory (DFT) with the use of the B3LYP functional.[40] For this purpose a split-valence 4-31G basis[41] was selected. The use of such a relatively small atomic basis set was mainly imposed by the huge number of energy minimisations required for an exhaustive sampling of the hypersurfaces. The above calculations have been termed B3LYP/4-31G. Several critical points were located by using a standard analytical-gradient based method as implemented in Gaussian 98.[42] Hessian matrices were then diagonalized in order to evaluate the actual nature of the potential energy saddle points, *i.e.* true minima, first or higher order stationary points. In correspondence with the deepest minima, with the use of their harmonic frequencies and moments of inertia, the thermal corrections to the energies as well as the entropic contributions were then calculated at 298 K in the ideal gas approximation. Finally the B3LYP/4-31G total energies were improved with single point calculations carried out using the larger 6-31G(d) basis set.[43] The above calculations have been termed B3LYP/6-31G(d)//B3LYP/4-31G.

The minima previously located in the vacuum calculations were then re-optimized using the polarizable continuum model. The solvents in such a model are represented by an infinite dielectric medium at the temperature of interest, *i.e.* 298 K. The cavity including the solute, defined in terms of interlocking spheres, is built with the GePol procedure[44] using the UAHF atomic radii.[45] The free energy of solvation is therefore evaluated in correspondence with the located minima by considering the electrostatic contribution (ΔGel), *i.e.* the solvation free energy arising from the electrostatic solute–solvent interaction, the cavitation contribution (ΔGcav) calculated through Pierotti's scaled particle theory[46] and the dispersion–repulsion contribution (ΔGdr).[47] All these calculations were carried out at a final B3LYP/6-31G(d)//B3LYP/4-31G level of theory.

The 298 K free energy differences between all the conformers were finally calculated through standard thermodynamic cycles involving the gaseous and solvated species using the ΔG_{298} in vacuum and in solution. It should be remarked that the present free energy calculations suffer from essentially two important limitations: the solvation model was not improved by adding a number of explicit solvent molecules and, most importantly, a meaningful evaluation of the molecular partition function cannot be derived with the presently available implementations of the PCM. Nevertheless, the error induced by this latter limitation is always assumed to be not dramatic.

Experimental measurements

Melting points were determined with a Büchi oil bath apparatus and are uncorrected. Optical rotations were taken at 20 °C with a Schmidt-Haensch Polartronic D polarimeter in a 1 dm cell (*c* 1.0 in $CHCl_3$). Infrared spectra were recorded with a Perkin-Elmer Spectrum 1000 FT-IR spectrometer (0.5, 2, and 3 mm NaCl cells). ^{1}H NMR spectra were measured with a Bruker AM 200 spectrometer in $CDCl_3$ solution, unless otherwise specified (tetramethylsilane as internal standard). *J* values are given in Hz. NOESY spectra were recorded in $CDCl_3$ and, in the case of compounds **2a**,**b**, also in DMSO-d_6 on an Avance 2000 Bruker console with a 1200-ms mixing time and displayed in the phase-sensitive mode. Usually 256 × 1024 data points were collected and for each block 64 transients were collected for two-dimensional experiments. The data sets were linearly predicted to 512 × 1024 data points. A Gaussian window was applied in both dimensions. Zero filling was used for a final spectrum size of 1024 × 1024 data points. Elemental analyses were performed at the Microanalysis Centre (Area della Ricerca di Roma, CNR, Montelibretti, Italy). Column chromatography was carried out using Merck silica gel 60 (230–400 mesh). Thin layer chromatography was performed on silica gel Merck 60 F254 plates. The drying agent was sodium sulfate. All reagents and solvents were purchased at highest commercial quality and used without further purification. Light petroleum refers to the 40–60 °C bp fraction.

N-Boc-Adt-Leu-OMe (1a)

To a solution of *N*-Boc-Adt-OMe[19] (0.100 g, 0.358 mmol) in MeOH (1.5 cm^3) 2 M NaOH (0.36 cm^3) was added under stirring. After 6 h at room temperature, the solution was

concentrated under vacuum, acidified with 0.5 M HCl, and extracted with EtOAc; the organic phase was washed with water, dried, and evaporated. To the residue, dissolved in DMF (3.0 cm^3) and cooled to 0 °C, HOBt (0.051 g, 0.376 mmol) and EDC (0.072 g, 0.376 mmol) were added. After stirring for 15 min at 0 °C and for 20 min at room temperature, H-Leu-OMe·HCl (0.072 g, 0.394 mmol) and TEA (0.055 cm^3, 0.394 mmol) were added. The reaction mixture was stirred at room temperature for 18 h and then diluted with water and extracted with EtOAc. The organic phase was washed with water, 10% citric acid solution, saturated $NaHCO_3$, and water, dried, and evaporated under reduced pressure. The residue (0.149 g) was chromatographed on silica gel (4.5 g) using $CHCl_3$ as eluent to give title dipeptide **1a** (0.125 g, 89%), mp 213–214 °C (from acetone). (Found: C, 48.9; H, 7.1. $C_{16}H_{28}N_2O_5S_2$ requires C, 49.0; H, 7.2%); $[\alpha]_D = -44°$; $\nu_{max}(CHCl_3)/cm^{-1}$ 3419, 1722, 1684, 1471, and 1157; ^1H NMR: δ 0.94 [6H, m, $CH(CH_3)_2$], 1.45 [9H, s, $C(CH_3)_3$],1.44–1.75 [3H, m, CH_2-$CH(CH_3)_2$], 3.34–3.80 (4H, m, two Adt β-CH_2), 3.73 (3H, s, $COOCH_3$), 4.63 (1H, m, Leu α-CH), 5.25 (1H, s, NH-COO), 7.03 (1H, d, *J* 8, Leu NH).

N-Boc-Ac$_5$c-Leu-OMe (1b)

To a solution of *N*-Boc-Ac$_5$c-OH (0.200 g, 0.873 mmol) in dry DMF (7.3 cm^3) cooled at 0 °C HOBt (0.124 g, 0.916 mmol) and EDC (0.176 g, 0.916 mmol) were added. After stirring 15 min at 0 °C H-Leu-OMe·HCl (0.175 g, 0.960 mmol) and TEA (0.134 cm^3, 0.960 mmol) were added. The reaction mixture was stirred at room temperature for 19 h and then worked up as described for **1a** to give crude **1b** which was further purified by crystallization from diethyl ether (0.260 g, 84%), mp 160–161 °C. (Found: C, 60.7; H, 9.1. $C_{18}H_{32}N_2O_5$ requires C, 60.6; H, 9.0%); $[\alpha]_D = -18°$; $\nu_{max}(CHCl_3)/cm^{-1}$ 3436, 3308, 1736, 1671, 1504, and 1161; ^1H NMR: δ 0.91 [6H, m, $CH(CH_3)_2$], 1.45 [9H, s, $C(CH_3)_3$],1.50–1.95 [9H, m, CH_2-$CH(CH_3)_2$, Ac$_5$c $C_\beta H_A$ and two γ-CH_2], 2.16–2.48 (2H, m, Ac$_5$c $C_\beta H_B$), 3.72 (3H, s, $COOCH_3$), 4.61 (1H, m, Leu α-CH), 4.80 (1H, s, NH-COO), 7.07 (1H, br, Leu NH).

HCO-Adt-Leu-OMe (2a)

A solution of **1a** (0.102 g, 0.26 mmol) in 1 cm^3 of formic acid was stirred at room temperature for 18 h. After removal of the excess of formic acid under vacuum, the residue was dissolved in dry DMF (0.7 cm^3) and EEDQ (0.078 g, 0.312 mmol) was added. The solution was stirred at room temperature for 24 h. Evaporation under reduced pressure afforded a residue (0.080 g) which was chromatographed on silica gel (5 g), eluting with $CHCl_3$–MeOH (99 : 1) to give pure **2a** (0.068 g, 82%), mp 72–73 °C (from CH_2Cl_2–*n*-hexane). (Found: C, 44.8; H, 6.2. $C_{12}H_{20}N_2O_4S_2$ requires C, 45.0; H, 6.3%); $[\alpha]_D = -29°$; ν_{max}(KBr)/cm^{-1} 3314, 1743, 1676, 1547, and 1212; ^1H NMR: δ 0.93 [6H, d, *J* = 5.9, $CH(CH_3)_2$], 1.57–1.70 [3H, m, CH_2-$CH(CH_3)_2$], 3.50–3.67 (4H, m, two Adt β-CH_2), 3.73 (3H, s, $COOCH_3$), 4.56 (1H, m, Leu α-CH), 6.49 (1H, s, Adt NH), 7.23 (1H, d, *J* 7.3, Leu NH), 8.25 (1H, d, *J* 1.3, HCO).

HCO-Ac$_5$c-Leu-OMe (2b)

A solution of **1b** (0.100 g, 0.28 mmol) in 0.7 cm^3 of formic acid was stirred at room temperature for 20 h. After removal of the excess of formic acid under vacuum, the residue was dissolved in dry DMF (1.2 cm^3) and EEDQ (0.083 g, 0.336 mmol) was added. The solution was stirred at room temperature for 18 h. Evaporation under reduced pressure afforded a residue (0.080 g) which was chromatographed on silica gel (5 g), eluting with $CHCl_3$–EtOAc (1 : 1) to give pure **2b** (0.070 g, 88%), mp 127–127.5 °C (from CH_2Cl_2–diethyl ether). (Found: C, 59.2; H, 8.4. $C_{14}H_{24}N_2O_4$ requires C, 59.1; H, 8.5%); $[\alpha]_D = -5°$; ν_{max}(KBr))/cm^{-1}: 3292, 1751, 1736, 1665, 1543, and 1157; ^1H NMR: δ 0.95 [6H, m, $CH(CH_3)_2$], 1.54–2.15 [9H, m, CH_2-$CH(CH_3)_2$, Ac$_5$c $C_\beta H_A$ and two γ-CH_2], 2.26–2.46 (2H, m, Ac$_5$c $C_\beta H_B$), 3.73 (3H, s, $COOCH_3$), 4.54 (1H, m, Leu α-CH), 5.84 (1H, s, Ac$_5$c NH), 7.25 (1H, d, *J* 7.3, Leu NH), 8.17 (1H, d, *J* 1.6, HCO).

N-Boc-Adt-Leu-Ala-OMe (3a)

To a solution of *N*-Boc-Leu-Ala-OMe[48] (0.113 g, 0.358 mmol) in dry MeOH (2.5 cm^3) cooled at 0 °C thionyl chloride (0.026 cm^3, 0.358 mmol) was added and the mixture was stirred at 50 °C for 3 h. Evaporation under reduced pressure of the solution afforded H-Leu-Ala-OMe·HCl which was used in the next step without further purification. To the stirred suspension of the hydrochloride in dry DMF (0.5 cm^3) cooled at 0 °C *N*-Boc-Adt-OH (0.095 g, 0.358 mmol), HOBt (0.048 g, 0.358 mmol), EDC (0.075 g, 0.358 mmol), and, after 15 min at 0 °C and 20 min at room temperature, TEA (0.050 cm^3, 0.358 mmol) were added. The mixture was stirred at room temperature for 16 h and then worked up as described for **1a** to give a residue (0.156 g) which, chromatographed on silica gel (5 g) using $CHCl_3$–EtOAc = 8 : 2 as eluent, afforded 0.131 g (79%) of **3a**, mp 154–155 °C (from acetone). (Found: C, 49.3; H, 7.1. $C_{19}H_{33}N_3O_6S_2$ requires C, 49.2; H, 7.2%); $[\alpha]_D = -27°$; $\nu_{max}(CHCl_3)/cm^{-1}$ 3415, 1716, 1627, 1504, and 1157; ^1H NMR: δ 0.92 [6H, m, $CH(CH_3)_2$], 1.40 (3H, d, *J* 7.2 Hz, Ala β-CH_3), 1.44 [9H, s, $C(CH_3)_3$], 1.55–1.76 [3H, m, CH_2-$CH(CH_3)_2$], 3.30–3.70 (4H, m, two Adt β-CH_2), 3.72 (3H, s, $COOCH_3$), 4.35–4.58 (2H, m, Ala and Leu α-CH), 5.26 (1H, s, NH-COO), 6.75 (1H, br, Ala NH), 6.85 (1H, d, *J* 7.7, Leu NH).

N-Boc-Ac$_5$c-Leu-Ala-OMe (3b)

To a solution of **1b** (0.346 g, 1 mmol) in MeOH (5.5 cm^3), 2 M NaOH (1 ml) was added under stirring. After 6 h at room temperature, the solution was concentrated under vacuum below 30 °C, acidified with 0.5 M HCl, and extracted with EtOAc; the organic phase was washed with water, dried, and evaporated. The resulting residue was used in the next step without further purification.

To the previous residue dissolved in DMF (5.5 cm^3) and cooled to 0 °C, HOBt (0.170 g, 1.1 mmol) and EDC (0.211 g, 1.1 mmol) were added. After stirring 15 min at 0 °C and 20 min at room temperature, H-Ala-OMe·HCl (0.154 g, 1.1 mmol) and TEA (0.155 cm^3, 1.1 mmol) were added. The reaction mixture was stirred at room temperature for 18 h and then worked up as described for **1a** to give a residue (0.42 g) which, chromatographed on silica gel (16 g) using CH_2Cl_2–EtOAc = 8 : 2 and 6 : 4 as eluent, afforded 0.341 g of the title product **3b** (80%), mp 140–141 °C (from EtOAc–light petroleum). (Found: C, 59.0; H, 8.8. $C_{21}H_{37}N_3O_6$ requires C, 59.0; H, 8.7%); $[\alpha]_D = -35°$; $\nu_{max}(CHCl_3)/cm^{-1}$ 3431, 1739, 1714, 1670, 1501, and 1161; ^1H NMR: δ 0.93 [6H, m, $CH(CH_3)_2$], 1.41 (3H, d, *J* 7.2 Hz, Ala β-CH_3), 1.44 [9H, s, $C(CH_3)_3$], 1.50–1.98 [9H, m, CH_2-$CH(CH_3)_2$, Ac$_5$c $C_\beta H_A$ and two γ-CH_2], 2.16–2.43 (2H, m, Ac$_5$c $C_\beta H_B$), 3.73 (3H, s, $COOCH_3$), 4.40–4.57 (2H, m, Ala and Leu α-CH), 4.85 (1H, s, NH-COO), 6.78 (1H, d, *J* 7.7, Leu NH), 6.98 (1H, br, Ala NH).

Abbreviations

B3LYP	hybrid functional for Density Functional Theory calculations
Boc	*tert*-butyloxycarbonyl
DCC	dicyclohexylcarbodiimide
DMF	*N*,*N*-dimethylformamide
DMSO	dimethyl sulfoxide
DRC	Dynamic Reaction Coordinate
EDC	*N*-(3-dimethylaminopropyl)-*N′*-ethylcarbodiimide hydrochloride
EEDQ	ethyl 2-ethoxy-1,2-dihydro-1-quinoline-carboxylate
EtOAc	ethyl acetate

f.e.	fully extended conformation
HOBt	1-hydroxybenzotriazole
MD	Molecular Dynamics
NMM	*N*-methylmorpholine
TEA	triethylamine
THF	tetrahydrofuran

Acknowledgements

We would like to thank Professor Alfredo Di Nola (University of Rome - La Sapienza) and CASPUR (Supercomputing Centre of Rome) for providing all the computational facilities.

References

1 C. Toniolo, M. Crisma, F. Formaggio and C. Peggion, *Biopolymers (Peptide Sciences)*, 2001, **60**, 396–419 and references therein.
2 P. Balaram, *Curr. Opin. Struct. Biol.*, 1992, **2**, 845–851.
3 C. Toniolo, *Janssen Chim. Acta*, 1993, **11**, 10–16.
4 P. Sudhanand, R. Balaji and P. Balaram, *Biopolymers*, 1995, **35**, 11–20.
5 I. Torrini, M. Paglialunga Paradisi, G. Pagani Zecchini and G. Lucente, *Synth. Commun.*, 1994, **24**, 153–158.
6 M. Cirilli, V. M. Coiro, A. Di Nola and F. Mazza, *Biopolymers*, 1998, **46**, 239–244.
7 C. Cativiela and M. D. Diaz-de-Villegas, *Tetrahedron: Asymmetry*, 1998, **9**, 3517–3599.
8 R. Kaul, S. Banumathi, D. Velmurugan, R. Balaji Rao and P. Balaram, *Biopolymers*, 2000, **54**, 159–167.
9 D. C. Horwell, *Bioorg. Med. Chem.*, 1996, **4**, 1573–1576.
10 I. Torrini, G. Pagani Zecchini, M. Paglialunga Paradisi, G. Lucente, G. Mastropietro, E. Gavuzzo, F. Mazza, G. Pochetti, S. Traniello and S. Spisani, *Biopolymers*, 1996, **39**, 327–337.
11 E. Mossel, F. Formaggio, M. Crisma, C. Toniolo, Q. B. Broxterman, W. H. J. Boesten, J. Kamphuis, P. J. L. M. Quaedflieg and P. Temussi, *Tetrahedron: Asymmetry*, 1997, **8**, 1305–1314.
12 I. Torrini, M. Paglialunga Paradisi, G. Pagani Zecchini, G. Lucente, E. Gavuzzo, F. Mazza, G. Pochetti, S. Traniello and S. Spisani, *Biopolymers*, 1997, **42**, 415–426.
13 A. G. S. Blommaert, H. Dhotel, B. Ducos, C. Durieux, N. Goudreau, A. Bado, C. Garbay and B. P. Roques, *J. Med. Chem.*, 1997, **40**, 647–658.
14 S. D. Bryant, R. Guerrini, S. Salvadori, C. Bianchi, R. Tomatis, M. Attila and L. H. Lazarus, *J. Med. Chem.*, 1997, **40**, 2579–2587.
15 C. Toniolo, *Int. J. Pept. Protein Res.*, 1990, **35**, 287–300.
16 M. Saviano, R. Iacovino, V. Menchise, E. Benedetti, G. M. Bonora, M. Gatos, L. Graci, F. Formaggio, M. Crisma and C. Toniolo, *Biopolymers*, 2000, **53**, 200–212.
17 C. Cativiela and M. D. Diaz-de-Villegas, *Tetrahedron: Asymmetry*, 2000, **11**, 645–732.
18 A. Moretto, F. Formaggio, M. Crisma, C. Toniolo, M. Saviano, R. Iacovino, R. M. Vitale and E. Benedetti, *J. Pept. Res.*, 2001, **57**, 307–315.
19 E. Morera, M. Nalli, F. Pinnen, D. Rossi and G. Lucente, *Bioorg. Med. Chem. Lett.*, 2000, **10**, 1585–1588 and references therein.
20 E. Morera, G. Lucente, G. Ortar, M. Nalli, F. Mazza, E. Gavuzzo and S. Spisani, *Bioorg. Med. Chem.*, 2002, **10**, 147–157.
21 E. Morera, F. Pinnen and G. Lucente, *Org. Lett.*, 2002, **4**, 1139–1142.
22 M. Paglialunga Paradisi, I. Torrini, G. Pagani Zecchini, G. Lucente, E. Gavuzzo, F. Mazza and G. Pochetti, *Tetrahedron*, 1995, **51**, 2379–2386.
23 T. P. Curran, N. M. Chandler, R. J. Kennedy and M. T. Keaney, *Tetrahedron Lett.*, 1996, **37**, 1933–1936.
24 A. F. Spatola, M. K. Anwer, A. L. Rockwell and L. M. Gierasch, *J. Am. Chem. Soc.*, 1986, **108**, 825–831.
25 A. M. Sapse, L. Mallah-Levy, S. B. Daniels and B. W. Erickson, *J. Am. Chem. Soc.*, 1986, **109**, 3256–3262.
26 K. Burgess and K. K. Ho, *J. Am. Chem. Soc.*, 1994, **116**, 799–805.
27 R. Haubner, R. Gracias, B. Diefenbach, S. L. Goodman, A. Jonczyk and H. Kessler, *J. Am. Chem. Soc.*, 1996, **118**, 7461–7466.
28 S. Herrero, M. T. Garcìa-Lòpez, M. Latorre, E. Cenarruzabeitia, J. Del Rio and R. Herranz, *J. Org. Chem.*, 2002, **67**, 3866–3873 and references therein.
29 L. Teuber, *Sulfur Rep.*, 1990, **9**, 257–349 and references therein.
30 J. J. P. Stewart, L. P. Davis and L. W. Burggraf, *J. Comput. Chem.*, 1987, **8**, 1117–1123.
31 M. J. S. Dewar and W. Thiel, *J. Am. Chem. Soc.*, 1977, **99**, 4999–5005.
32 See for example: R. Improta, N. Rega, C. Aleman and V. Barone, *Macromolecules*, 2001, **34**, 7550–7557.
33 S. Miertus, E. Scrocco and J. Tomasi, *J. Chem. Phys.*, 1981, **55**, 117–122.
34 J. Tomasi and M. Persico, *Chem. Rev.*, 1994, **94**, 2027–2035.
35 G. Lajoie and J. L. Kraus, *Peptides*, 1984, **5**, 563.
36 P. A. Ray and P. Balaram, *Biopolymers*, 1985, **24**, 1131–1146.
37 S. Zerkout, V. Dupont, A. Aubry, J. Vidal, A. Collet, A. Vicherat and A. Marraud, *Int. J. Pept. Protein Res.*, 1994, **44**, 378–387.
38 *Gamess* (version R1). M. W. Schmidt, K. K. Baldridge, J. A. Boatz, S. T. Elbert, M. S. Gordon, J. H. Jensen, S. Koseki, N. Matsunaga, K. A. Nguyen, S. J. Su and T. L. Windus, *J. Comput. Chem.*, 1993, **14**, 1347–1363.
39 M. P. Allen and D. J. Tildesley, *Computer Simulations of Liquids*, Oxford University Press, Oxford, 1987.
40 A. D. Becke, *J. Chem. Phys.*, 1992, **98**, 5648–5652.
41 R. Ditchfield, W. J. Hehre and J. A. Pople, *J. Chem. Phys.*, 1971, **54**, 724–728.
42 M. J. Frisch, G. W. Trucks, H. B. Schlegel, G. E. Scuseria, M. A. Robb, J. R. Cheeseman, V. G. Zakrzewski, J. A. Montgomery, Jr., R. E. Stratmann, J. C. Burant, S. Dapprich, J. M. Millam, A. D. Daniels, K. N. Kudin, M. C. Strain, O. Farkas, J. Tomasi, V. Barone, M. Cossi, R. Cammi, B. Mennucci, C. Pomelli, C. Adamo, S. Clifford, J. Ochterski, G. A. Petersson, P. Y. Ayala, Q. Cui, K. Morokuma, P. Salvador, J. J. Dannenberg, D. K. Malick, A. D. Rabuck, K. Raghavachari, J. B. Foresman, J. Cioslowski, J. V. Ortiz, A. G. Baboul, B. B. Stefanov, G. Liu, A. Liashenko, P. Piskorz, I. Komaromi, R. Gomperts, R. L. Martin, D. J. Fox, T. Keith, M. A. Al-Laham, C. Y. Peng, A. Nanayakkara, M. Challacombe, P. M. W. Gill, B. G. Johnson, W. Chen, M. W. Wong, J. L. Andres, C. Gonzalez, M. Head-Gordon, E. S. Replogle and J. A. Pople, GAUSSIAN 98 (Revision A.11), Gaussian, Inc., Pittsburgh, PA, 2001.
43 M. M. Francl, W. J. Petro, W. J. Hehre, J. S. Binkley, M. S. Gordon, D. J. DeFree and J. A. Pople, *J. Chem. Phys.*, 1982, **77**, 3654–3659.
44 J. Pasqual-Ahuir, E. Silla, J. Tomasi and R. Bonaccorsi, *J. Comput. Chem.*, 1996, **17**, 56–71.
45 V. Barone, M. Cossi and J. Tomasi, *J. Chem. Phys.*, 1997, **107**, 3210–3215.
46 R. A. Pierotti, *Chem. Rev.*, 1976, **76**, 717–730.
47 F. M. Floris and J. Tomasi, *J. Comput. Chem.*, 1986, **10**, 616–630.
48 K. Pudhom and T. Vilaivan, *Synth. Commun.*, 2001, **31**, 61–70.